ISSN 1738-6055 (Print)
ISSN 2233-7660 (Online)

Lab Anim Res 2018: 34(4), 264-269
https://doi.org/10.5625/lar.2018.34.4.264

Laboratory Animal Research
http://submission.kalas.or.kr

Generation of knockout mouse models of cyclin-dependent kinase inhibitors by engineered nuclease-mediated genome editing

Bo Min Park, Jae-il Roh*, Jaehoon Lee*, Han-Woong Lee*

Department of Biochemistry, College of Life Science & Biotechnology, Yonsei University, Seoul, Korea

Cell cycle dysfunction can cause severe diseases, including neurodegenerative disease and cancer. Mutations in cyclin-dependent kinase inhibitors controlling the G1 phase of the cell cycle are prevalent in various cancers. Mice lacking the tumor suppressors *p16*^{Ink4a} (*Cdkn2a*, cyclin-dependent kinase inhibitor 2a), *p19*^{Arf} (an alternative reading frame product of *Cdkn2a*,), and *p27*^{Kip1} (*Cdkn1b*, cyclin-dependent kinase inhibitor 1b) result in malignant progression of epithelial cancers, sarcomas, and melanomas, respectively. Here, we generated knockout mouse models for each of these three cyclin-dependent kinase inhibitors using engineered nucleases. The *p16*^{Ink4a} and *p19*^{Arf} knockout mice were generated via transcription activator-like effector nucleases (TALENs), and *p27*^{Kip1} knockout mice via clustered regularly interspaced short palindromic repeats/CRISPR-associated nuclease 9 (CRISPR/Cas9). These gene editing technologies were targeted to the first exon of each gene, to induce frameshifts producing premature termination codons. Unlike preexisting embryonic stem cell-based knockout mice, our mouse models are free from selectable markers or other external gene insertions, permitting more precise study of cell cycle-related diseases without confounding influences of foreign DNA.

Keywords: TALEN, CRISPR/Cas9, cyclin-dependent kinase inhibitor

Received 20 October 2018; Revised version received 7 December 2018; Accepted 8 December 2018

The cell cycle constitutes a series of events required for cell division, controlled by cyclin-dependent kinases (CDKs) and their inhibitors [3,14]. *Cdkn2a* (cyclin-dependent kinase inhibitor 2a) is a cell cycle regulating gene encoding alternate proteins, p16^{Ink4a} and p19^{Arf}, that arrest the G1 phase through CDK4/6 inhibition [10,12]. As they are tumor suppressors, p16^{Ink4a} and p19^{Arf} can be targeted for treatment of various cancers, including melanoma, cervical, and esophageal cancers [4,13,22, 30,32]. p27^{Kip1} is another type of CDK inhibitor which suppresses CDK2, a CDK required for S phase entry [23]. Orchestration of these kinases and their inhibitors controls the cell cycle; therefore, mutations in these proteins can cause severe disease [16,25,33]. For these reasons, knockout (KO) mouse models for these genes have been generated and extensively studied for almost three decades [2,26].

The use of engineered nucleases, such as transcription activator-like effector nucleases (TALENs) and clustered regularly interspaced short palindromic repeats/CRISPR-associated nuclease 9 (CRISPR/Cas9), can tremendously reduce the time and cost required for mouse model production [11,28,29]. TALENs consist of transcription activator-like (TAL) effectors fused with a FokI cleavage domain [9]. Each TAL effector can be engineered to recognize specific DNA sequences by customizing the

*Corresponding authors: Han-Woong Lee, Department of Biochemistry, College of Life Science & Biotechnology and Yonsei Laboratory Animal Research Center, Yonsei University, Seoul 03722, Korea
Tel: +82-2-2123-5698; Fax: +82-2-2123-8107; E-mail: hwl@yonsei.ac.kr
Jaehoon Lee, Department of Biochemistry, College of Life Science & Biotechnology and Yonsei Laboratory Animal Research Center, Yonsei University, Seoul 03722, Korea
Tel: +82-2-2123-7642; Fax: +82-2-2123-8107; E-mail: jhlee13@gmail.com
Jae-il Roh, Department of Biochemistry, College of Life Science & Biotechnology, Yonsei University, Seoul 03722, Korea
Tel: +82-2-2123-7642; Fax: +82-2-2123-8107; E-mail: rohjaeil@gmail.com

amino acids at the 12th and 13th position of each ~34 amino acid repeat in the protein's variable region [6]. CRISPR/Cas9 is a ribonucleoprotein complex, containing a single guide RNA (sgRNA) with a targeting sequence and a Cas9 protein which recognizes a protospacer adjacent motif and cleaves the target site [24].

To better understand the mechanisms by which CDK inhibitors influence tumor progression, and to permit study without any intervening patent or authority, we established KO mouse models for $p16^{Ink4a}$, $p19^{Arf}$, and $p27^{Kip1}$. While previous mouse models were generated using homologous recombination in embryonic stem (ES) cells [17,26], ours utilized TALEN- and CRISPR/Cas9 to induce indels via non-homologous end joining repair. These nuclease-mediated approaches permitted generation of KOs without the addition of exogenous genes, such as a neomycin resistance (Neo^R) cassette. KO models for each gene were established in both C57BL/6JBomTac (B6) and FVB/NTac (FVB) genetic backgrounds.

Materials and Methods

In vitro synthesis of TALENs, Cas9 mRNA, and sgRNAs

RNAs for TALENs and CRISPR/Cas9 were prepared as described previously [5,21,27]. Briefly, TALEN and *Cas9* mRNAs were synthesized *in vitro* from linear DNA templates (ToolGen, Korea) via the mMESSAGE mMACHINE T7 Ultra kit (Invitrogen, USA) according to the manufacturer's instructions. DNA templates for sgRNAs were synthesized *in vitro* by PCR. The sgRNAs were produced from these templates using a MEGA-shortscript T7 kit (Invitrogen, USA) according to the manufacturer's instructions. The sgRNAs were diluted in RNase-free injection buffer (0.25 mM EDTA, 10 mM Tris at pH 7.4) and introduced into the cytoplasm of fertilized eggs by microinjection. TALEN target sites were as follows: TALEN #1 for p16, 5'-TGCATGACGT GCGGGCACTG-3'; TALEN #2 for p16, 5'-TTCGGGG CGTTGGGCGAAAC-3' for both B6 and FVB mice; TALEN #1 of p19, 5'-TTCGTGCGATCCCGGAGACC-3'; TALEN #2 of p19, 5'-TCACGAAAGCCAGAGCGC AG-3' for both B6 and FVB mice. The following sequences were used for sgRNA synthesis: sgRNA #1 of p27, 5'-GCGGATGGACGCCAGACAAG-3'; sgRNA #2 of p27, 5'-GGACTTGGAGAAGCACTGCC-3'.

Generation and maintenance of p16, p19, and p27 KO mice

$p16^{Ink4a}$, *$p19^{Arf}$*, and *$p27^{Kip1}$* KO mice were established using engineered nucleases as described previously [21]. Briefly, TALENs or Cas9/sgRNAs were microinjected into the fertilized embryos of B6 and FVB mice. Mutations in the target genes were confirmed by Sanger sequencing (BIONICS, Korea). Mice were maintained on a normal chow diet under a twelve-hour (8:00-20:00 light) light/dark cycle at the specific-pathogen-free facility. All animal experiments were held in accordance with Korean Food and Drug Administration guidelines, and protocols were approved by the Institutional Animal Care and Use Committee of the Yonsei University (201507-390-01).

Genotyping of KO mice

Mouse genotypes were confirmed by PCR using the following primers: 5'-GTTTAATGGGTGGCTCCGGT-3' (p16-B6-KO-F), 5'-TTGGGCGAAACCCCAGC-3' (p16-B6-KO-R) resulting 443 bps, 5'-CGTGCGGGCAC TGCTGGAAGCCGG-3' (p16-B6-WT-F), 5'-GGTGTT AGCGTGGGTAGCAG-3' (p16-B6-WT-R) resulting 198 bps, 5'-GAGGAGAGCCATCTGGAG-3' (p16-FVB-F), 5'-CCTTGCCTACCTGAATCG-3' (p16-FVB-R) resulting 158 bps for WT and 133 bps for KO; 5'-AGGGTTTTCTTGGTGAAGTTC-3' (p19-B6-F), 5'-TC CTCTCTAGCCTCAACAAC-3' (p19-B6-R) resulting 94 bps for WT and 72 bps for KO, 5'-GCTTCTCACCT CGCTTGTC-3' (p19-FVB-F), 5'-GAGCGCAGCTCGCG-3' (p19-FVB-R WT), and 5'-AGAGCGCAGCTCGCTG-3' (p19-FVB-R KO) resulting 200 bps for both WT and KO specific; 5'-CGCTTTTGTTCGGTTTTGTT-3' (p27-F), 5'-CTCTCCACCTCCTGCCAC-3' (p27-R) resulting 180 bps for WT and 94 bps for KO. PCR was performed as described previously [19] at the following annealing temperatures: p16 KO, 56ºC for B6 and 58ºC for FVB; p19 KO, 60ºC for both B6 and FVB; p27 KO, 56ºC for B6 and 68ºC for FVB. Electrophoresis was conducted on 2-3% agarose gels and visualized with a Bio-Rad ChemiDoc system (Bio-Rad, USA).

Western blotting

Protein lysates were prepared as described previously [20]. Briefly, cell lysates were prepared in RIPA lysis buffer containing protease inhibitor cocktail. Antibodies

raised against p16 (sc-377412, Santa Cruz Biotechnology, USA) and ACTIN (sc-58673, Santa Cruz Biotechnology, USA) were used for detection via Western blot.

Results

Generation of p16^{Ink4a} and p19^{Arf} KO mice using TALENs

Cdkn2a is a cell cycle regulating gene that encodes two different proteins, called p16^{Ink4a} and p19^{Arf}, through exon 1 variants [26,33]. To establish the *p16^{Ink4a}* KO mouse model in the FVB background, a pair of TALEN RNAs targeting exon 1 of *p16^{Ink4a}* was synthesized and microinjected into the mouse embryos. An FVB-*p16^{Ink4a}* KO mouse line possessing a 25 bp deletion downstream of the start codon (Figure 1A) was selected via PCR-based screening and Sanger sequencing. The resulting mutant *p16^{Ink4a}* gene is predicted to encode only 11 amino acids (AAs) downstream of the mutation site, due to a frameshift-induced premature termination codon (PTC). Including sequence upstream of the mutation site, the truncated protein is predicted to include 34 AAs, compared to 168 AAs in the WT p16^{Ink4a} protein. Importantly, the PTC in the mutated transcripts may cause nonsense-mediated mRNA decay (NMD), resulting in remarkable reduction of mutant mRNA levels [18]. The genotypes of *p16^{Ink4a}* KO mice were confirmed by PCR, and its products were represented in 158 bp for WT and 133 bp for KO (Figure 1C). The same strategy was applied to establish the B6-*p16^{Ink4a}* KO in the C57BL/6 strain, which generated a mouse line harboring a seven-nucleotide deletion predicted to produce abnormal 16 AAs before a PTC (Figure 1B), leading to NMD-mediated mRNA degradation or translation of a predicted 40 AA peptide. In contrast, the WT p16^{Ink4a} protein is 168 AA in length. The genotyping PCR products represented in 443 bp for WT and in 198 bp for KO mice (Figure 1D). Immunoblot assays were conducted

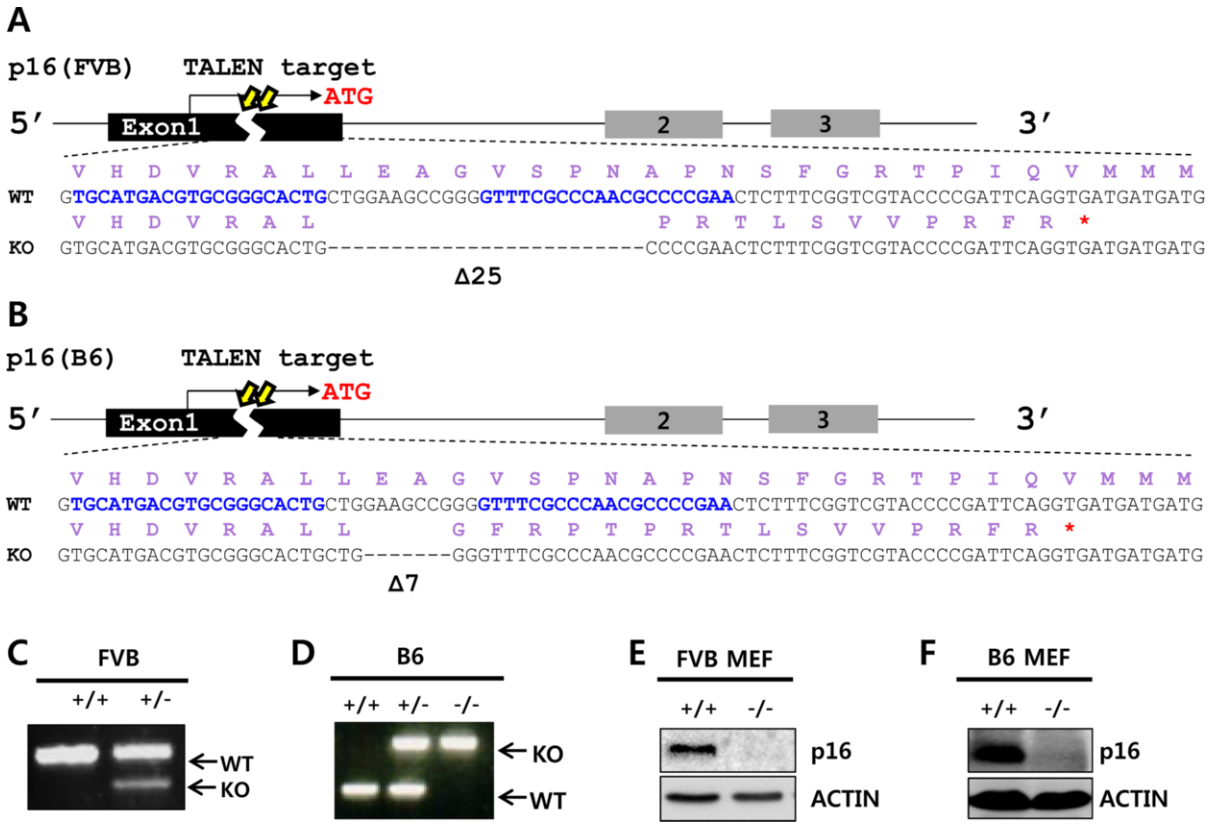

Figure 1. TALEN-mediated generation of a *p16^{Ink4a}* knockout mouse model. (A and B) Representative views of the transcription activator-like effector nuclease (TALEN) targeting strategy for generation of *p16^{Ink4a}* KO mice in both FVB (A) and B6 (B) strains. A schematic of the *Cdkn2a* locus with TALEN-binding nucleotides (blue) and the amino acid sequences (purple) of the WT (upper) and KO (lower) mice are shown. *p16^{Ink4a}* exons are indicated with boxes and introns are indicated by lines. Red asterisks indicate stop codons. (C and D) Representative results of PCR genotyping for FVB (C) and C57BL/6 (D) strains of WT and *p16^{Ink4a}* KO mice. +/+, WT; +/-, Heterozygote KO; -/-, Homozygote KO. (E and F) Western blot analyses for p16 in FVB (E) and B6 (F) mouse embryonic fibroblasts. +/+ indicates WT and -/- indicates the *p16^{Ink4a}* KO.

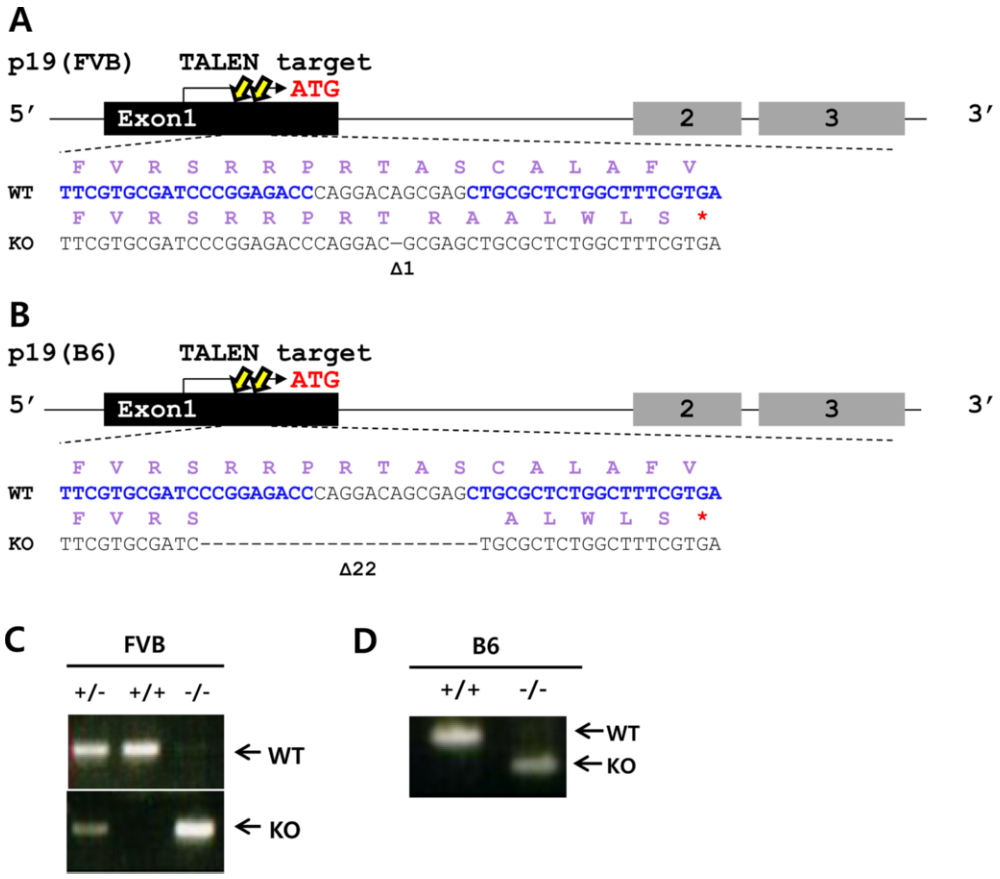

Figure 2. TALEN-mediated generation of a *p19*^{Arf} knockout mouse model. (A and B) Representative views of the transcription activator-like effector nuclease (TALEN) targeting strategy for generation of *p19*^{Arf} KO mice in both FVB (A) and B6 (B) strains. A schematic of the *Cdkn2a* locus with TALEN-binding nucleotides (blue) and the amino acid sequences (purple) of the WT (upper) and KO (lower) mice are shown. *p19*^{Arf} exons are indicated with boxes and introns are indicated by lines. Red asterisks indicate stop codons. (C and D) Representative results of PCR genotyping for FVB (C) and B6 (D) strains of WT and *p19*^{Arf} KO mice. +/+, WT; +/-, Heterozygote KO; -/-, Homozygote KO.

to examine p16^{Ink4a} protein levels in mouse embryonic fibroblasts (MEFs). Ablation of p16^{Ink4a} protein was detected in *p16*^{Ink4a} KO MEFs in both FVB and B6 strains (Figures 1E and F), indicating that TALEN-induced *p16*^{Ink4a} mutations successfully eliminated gene expression.

To produce the *p19*^{Arf} KO mouse model, a strategy similar to the *p16*^{Ink4a} KOs was deployed. One and twenty-two bp deletion mutants were generated that may produce only seven and five aberrant AAs downstream of the mutation sites in FVB and B6 strains, respectively. The mutant transcripts may undergo NMD or generate peptides 43 AAs in length in FVB and 36 AAs in length in B6 (Figures 2A and B). The genotypes were confirmed by genotyping PCR. In the case of FVB *p19*^{Arf} KO mouse, the PCR product size for WT and KO were identical at 200 bp, therefore they were verified in different agarose gels. Whereas the genotyping PCR products in the B6 *p19*^{Arf} KO mouse represented in 94 bp for WT and in 72 bp for KO (Figures 2C and D). Notably, previous *p16*^{Ink4a} and *p19*^{Arf} KO mouse models were established by replacing the exon(s) with a Neo^{R}-cassette in ES cells [26], whereas our *Cdkn2a* KO mice are Neo^{R}-free.

Generation of B6 *p27*^{Kip1} KO mice by CRISPR/Cas9 microinjection

To establish the mouse model for p27^{Kip1}, two sgRNAs targeting the first exon of were designed using sgRNA design tools to maximize on-target and minimize off-target activity [7,8]. The sgRNAs were synthesized and microinjected with *Cas9* mRNA into the mouse embryos to cause mutations at the target sites (Figure 3). Through PCR-based genotyping and Sanger sequencing, we selected a mutant line harboring an 86 bp deletion between the target sites (Figure 3A), resulting in the

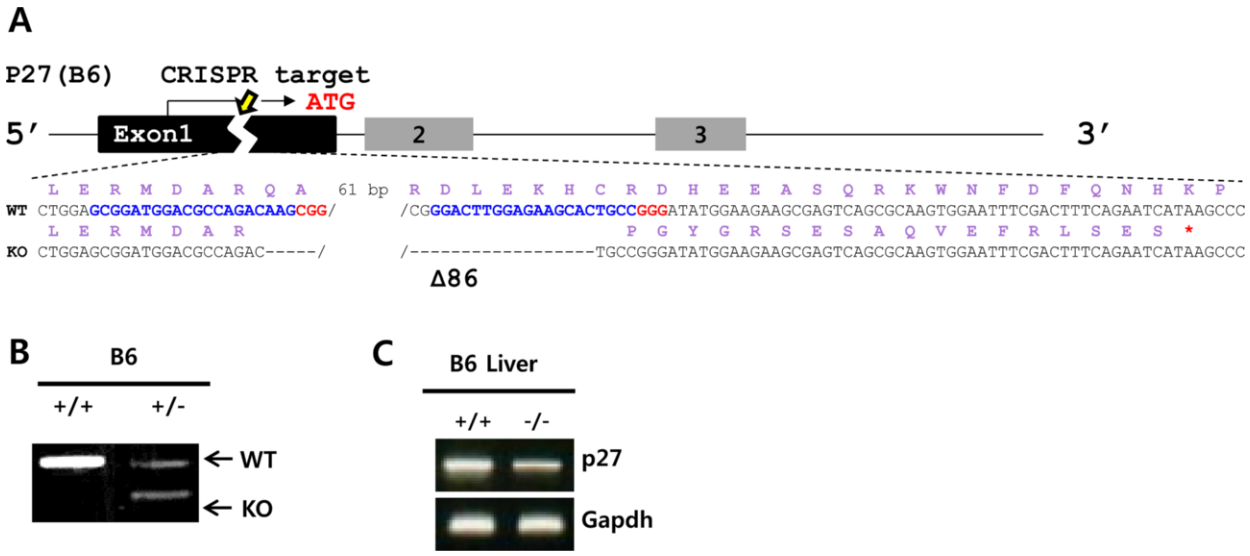

Figure 3. CRISPR/Cas9-mediated generation of B6-*p27*^{Kip1} knockout mouse model. (A) Representative view of the clustered regularly interspaced short palindromic repeats/CRISPR-associated nuclease 9 (CRISPR/Cas9) targeting strategy for generation of *p27*^{Kip1} KO mouse. A schematic of the *Cdkn1b* locus with single guide RNA target nucleotides (blue) and the amino acid sequences (purple) of the wild-type (upper) and knockout (lower) mice are shown. Exons are indicated with boxes and introns are indicated by lines. Red asterisks indicate stop codons. The protospacer adjacent motif for Cas9 is indicated in red. (B) A representative result of PCR genotyping for B6 strain of WT and *p27*^{Kip1} KO mouse. +/+, WT; +/-, Heterozygote KO. (C) Semi-quantitative PCR analysis for *p27* transcript in the liver of WT and *p27*^{Kip1} KO mouse. +/+, WT; -/-, Homozygote *p27*^{Kip1} KO.

probable translation of 18 abnormal peptides downstream of the deletion site, followed by a PTC. Compared to WT *p27*^{Kip1}, which encodes 198 AAs, the *p27*^{Kip1} KO in B6 strain is predicted to produce only 39 AAs, if not completely silenced via NMD. The genotyping PCR products represented in 180 bp for WT and 94 bp for KO (Figure 3B). Although some reduced RNA was detected in the liver of *p27*^{Kip1} KO mouse, the verified genetic alteration ensured that a functional protein will not be expressed (Figure 3C).

Discussion

The KO mouse models we established possess small deletions in the first exon of each gene, leading to frameshift-mediated PTCs in the open reading frame of the genes. In addition to premature truncation, the introduced mutations may cause NMD of mutant mRNAs. NMD is a mRNA quality control mechanism that monitors translation and degrades mutant mRNA harboring PTC [18]. Therefore, expression of the targeted CDK inhibitors should be considerably decreased in their respective KO mice. The KO mice in this study will be helpful for further studies in areas such as cellular senescence, tumorigenesis, cataracts, and co-orchestration with oncogenes and tumor suppressors [15,26], without potential interference from external genes (e.g. Neo^{R}). The Neo^{R} marker has been shown to affect glycolysis rate, induce C-MYC (which is frequently overexpressed in primary tumors), and suppress various genes by acting as a transcriptional silencer [1,31]. To avoid adverse effects and biased phenotypes, we generated KO mice lacking this cassette. Collectively, these models will be useful tools for the study of diseases associated with CDK inhibitor deficiency. All of these newly established models are available from the Korean Ministry of Food & Drug Safety (www.nifds.go.kr) to support biomedical research.

Acknowledgments

This work was supported by the National Research Foundation of the Republic of Korea (grants 2015R1A2A1A01003845 and 2017R1A4A1015328) and Korea's Ministry of Food and Drug Safety (MFDS, 14182 MFDS978).

Conflict of interests The authors declare that there is no financial conflict of interests to publish these results.

References

1. Artelt P, Grannemann R, Stocking C, Friel J, Bartsch J, Hauser H. The prokaryotic neomycin-resistance-encoding gene acts as a transcriptional silencer in eukaryotic cells. Gene 1991; 99(2): 249-254.
2. Baker DJ, Perez-Terzic C, Jin F, Pitel KS, Niederländer NJ, Jeganathan K, Yamada S, Reyes S, Rowe L, Hiddinga HJ, Eberhardt NL, Terzic A, van Deursen JM. Opposing roles for p16Ink4a and p19Arf in senescence and ageing caused by BubR1 insufficiency. Nat Cell Biol 2008; 10(7): 825-836.
3. Besson A, Dowdy SF, Roberts JM. CDK inhibitors: cell cycle regulators and beyond. Dev Cell 2008; 14(2): 159-169.
4. Capparelli C, Chiavarina B, Whitaker-Menezes D, Pestell TG, Pestell RG, Hulit J, Andò S, Howell A, Martinez-Outschoorn UE, Sotgia F, Lisanti MP. CDK inhibitors (p16/p19/p21) induce senescence and autophagy in cancer-associated fibroblasts, "fueling" tumor growth via paracrine interactions, without an increase in neo-angiogenesis. Cell Cycle 2012; 11(19): 3599-3610.
5. Choi JY, Yun WB, Kim JE, Lee MR, Park JJ, Song BR, Kim HR, Park JW, Kang MJ, Kang BC, Lee HW, Hwang DY. Successful development of squamous cell carcinoma and hyperplasia in RGEN-mediated p27 KO mice after the treatment of DMBA and TPA. Lab Anim Res 2018; 34(3): 118-125.
6. Deng D, Yan C, Pan X, Mahfouz M, Wang J, Zhu JK, Shi Y, Yan N. Structural basis for sequence-specific recognition of DNA by TAL effectors. Science 2012; 335(6069): 720-723.
7. Doench JG, Fusi N, Sullender M, Hegde M, Vaimberg EW, Donovan KF, Smith I, Tothova Z, Wilen C, Orchard R, Virgin HW, Listgarten J, Root DE. Optimized sgRNA design to maximize activity and minimize off-target effects of CRISPR-Cas9. Nat Biotechnol 2016; 34(2): 184-191.
8. Hsu PD, Scott DA, Weinstein JA, Ran FA, Konermann S, Agarwala V, Li Y, Fine EJ, Wu X, Shalem O, Cradick TJ, Marraffini LA, Bao G, Zhang F. DNA targeting specificity of RNA-guided Cas9 nucleases. Nat Biotechnol 2013; 31(9): 827-832.
9. Joung JK, Sander JD. TALENs: a widely applicable technology for targeted genome editing. Nat Rev Mol Cell Biol 2013; 14(1): 49-55.
10. Kurokawa K, Tanaka T, Kato J. p19ARF prevents G1 cyclin-dependent kinase activation by interacting with MDM2 and activating p53 in mouse fibroblasts. Oncogene 1999; 18(17): 2718-2727.
11. Lee JH, Rho JI, Devkota S, Sung HY, Lee HW. Developing genetically engineered mouse models using engineered nucleases: Current status, challenges, and the way forward. Drug Discov Today 2016; 20: 13-20.
12. Li J, Poi MJ, Tsai MD. Regulatory mechanisms of tumor suppressor P16(INK4A) and their relevance to cancer. Biochemistry 2011; 50(25): 5566-5582.
13. Liggett WH Jr, Sidransky D. Role of the p16 tumor suppressor gene in cancer. J Clin Oncol 1998; 16(3): 1197-1206.
14. Lim S, Kaldis P. Cdks, cyclins and CKIs: roles beyond cell cycle regulation. Development 2013; 140(15): 3079-3093.
15. McKeller RN, Fowler JL, Cunningham JJ, Warner N, Smeyne RJ, Zindy F, Skapek SX. The Arf tumor suppressor gene promotes hyaloid vascular regression during mouse eye development. Proc Natl Acad Sci U S A 2002; 99(6): 3848-3853.
16. Nagy Z. The dysregulation of the cell cycle and the diagnosis of Alzheimer's disease. Biochim Biophys Acta 2007; 1772(4): 402-408.
17. Nakayama K, Ishida N, Shirane M, Inomata A, Inoue T, Shishido N, Horii I, Loh DY, Nakayama K. Mice lacking p27(Kip1) display increased body size, multiple organ hyperplasia, retinal dysplasia, and pituitary tumors. Cell 1996; 85(5): 707-720.
18. Popp MW, Maquat LE. Leveraging Rules of Nonsense-Mediated mRNA Decay for Genome Engineering and Personalized Medicine. Cell 2016; 165(6): 1319-1322.
19. Roh JI, Cheong C, Sung YH, Lee J, Oh J, Lee BS, Lee JE, Gho YS, Kim DK, Park CB, Lee JH, Lee JW, Kang SM, Lee HW. Perturbation of NCOA6 leads to dilated cardiomyopathy. Cell Rep 2014; 8(4): 991-998.
20. Roh JI, Kim Y, Oh J, Kim Y, Lee J, Lee J, Chun KH, Lee HW. Hexokinase 2 is a molecular bridge linking telomerase and autophagy. PLoS One 2018; 13(2): e0193182.
21. Roh JI, Lee J, Park SU, Kang YS, Lee J, Oh AR, Choi DJ, Cha JY, Lee HW. CRISPR-Cas9-mediated generation of obese and diabetic mouse models. Exp Anim 2018; 67(2): 229-237.
22. Romagosa C, Simonetti S, López-Vicente L, Mazo A, Lleonart ME, Castellvi J, Ramon y Cajal S. p16(Ink4a) overexpression in cancer: a tumor suppressor gene associated with senescence and high-grade tumors. Oncogene 2011; 30(18): 2087-2097.
23. Sa G, Guo Y, Stacey DW. The regulation of S phase initiation by p27Kip1 in NIH3T3 cells. Cell Cycle 2005; 4(4): 618-627.
24. Sander JD, Joung JK. CRISPR-Cas systems for editing, regulating and targeting genomes. Nat Biotechnol 2014; 32(4): 347-355.
25. Shankland SJ. Cell-cycle control and renal disease. Kidney Int 1997; 52(2): 294-308.
26. Sharpless NE, Ramsey MR, Balasubramanian P, Castrillon DH, DePinho RA. The differential impact of p16(INK4a) or p19(ARF) deficiency on cell growth and tumorigenesis. Oncogene 2004; 23(2): 379-385.
27. Sung YH, Baek IJ, Kim DH, Jeon J, Lee J, Lee K, Jeong D, Kim JS, Lee HW. Knockout mice created by TALEN-mediated gene targeting. Nat Biotechnol 2013; 31(1): 23-24.
28. Sung YH, Jin Y, Kim S, Lee HW. Generation of knockout mice using engineered nucleases. Methods 2014; 69(1): 85-93.
29. Sung YH, Kim JM, Kim HT, Lee J, Jeon J, Jin Y, Choi JH, Ban YH, Ha SJ, Kim CH, Lee HW, Kim JS. Highly efficient gene knockout in mice and zebrafish with RNA-guided endonucleases. Genome Res 2014; 24(1): 125-131.
30. Ulanet DB, Hanahan D. Loss of p19(Arf) facilitates the angiogenic switch and tumor initiation in a multi-stage cancer model via p53-dependent and independent mechanisms. PLoS One 2010; 5(8): e12454.
31. Valera A, Perales JC, Hatzoglou M, Bosch F. Expression of the neomycin-resistance (neo) gene induces alterations in gene expression and metabolism. Hum Gene Ther 1994; 5(4): 449-456.
32. Weber JD, Jeffers JR, Rehg JE, Randle DH, Lozano G, Roussel MF, Sherr CJ, Zambetti GP. p53-independent functions of the p19(ARF) tumor suppressor. Genes Dev 2000; 14(18): 2358-2365.
33. Zhivotovsky B, Orrenius S. Cell cycle and cell death in disease: past, present and future. J Intern Med 2010; 268(5): 395-409.